IEEE Access
Multidisciplinary | Rapid Review | Open Access Journal

Received June 21, 2021, accepted July 17, 2021, date of publication July 26, 2021, date of current version July 30, 2021.

Digital Object Identifier 10.1109/ACCESS.2021.3099462

A Manchester-OOK Visible Light Communication System for Patient Monitoring in Intensive Care Units

KLAAS MINNE VAN DER ZWAAG[1], MARIANNE PONTARA MARINHO[1], WESLEY DA SILVA COSTA[1], FRANCISCO DE ASSIS SOUZA DOS SANTOS[2], TEODIANO FREIRE BASTOS-FILHO[1], HELDER R. O. ROCHA[1], MARCELO E. V. SEGATTO[1], AND JAIR A. L. SILVA[1], (Member, IEEE)

[1]Postgraduate Program in Electrical Engineering, Federal University of Espírito Santo, Vitória-ES, 29075910, Brazil
[2]Department of Computing and Electronics, Federal University of Espírito Santo, São Mateus, Vitória-ES, 29060970, Brazil

Corresponding author: Jair A. L. Silva (jair.silva@ufes.br)

This work was supported in part by the PRONEX/Fundação de Amparo à Pesquisa e Inovação do Espírito Santo (FAPES)-280/2018, in part by the FAPES-538/2018, in part by the FAPES-601/2018, in part by the FAPES/Conselho Nacional de Desenvolvimento Científico e Tecnológico (CNPq)-84343338 (Programa De Pesquisa Para o SUS: Gestão Compartilhada Em Saúde), in part by the CNPq-307757/2016-1, in part by the CNPq-304564/2016-8, in part by the CNPq-309823/2018-8, and in part by the Núcleo de Investigação e Pesquisa Pró-Africa (NiDa) Projects.

ABSTRACT Visible Light Communication (VLC) is an interesting solution in Intensive Care (IC) medical environments to, among others, prevent the spread of emerging diseases. This work presents the design of a low-cost and stable VLC transceiver system in addition to practical characterizations and experimental performance evaluations for application in IC environments. The application focuses on the transmission of Manchester-based on-off keying signals, in a proof-of-concept apparatus that makes use of the Eye Opening Penalty (EOP) metric to illustrate a comprehensive picture of the potentials of the evaluated VLC system. Parameters such as Light-Emitting Diode (LED) bias current, modulation frequency, line-of-sight link distance, and signal pattern were analyzed here. Experimental results show an outstanding behavior considering an LED bias current of 400 mA, a signal frequency of 1 MHz and a VLC transmission link length of 2.5 m. To validate our system, vital parameters as heart rate, oxygen saturation, pulse rate, respiration rate, temperature and non-intrusive blood pressure signals were transmitted for VLC links of 1.5, 5 and 15 m, which were received by a multi-parameter monitor, with EOP values of 0.89, 0.96 and 2.67 dB, respectively.

INDEX TERMS E-health, intensive care environments, visible light communication, manchester coding.

I. INTRODUCTION

The increasing demand for wireless links with high-reliable and low latency require modern wireless technologies predicted in 5G and beyond [1], [2]. The gradually exhausting radio frequency (RF) resources have encouraged scientific investigations on alternative wireless technologies to, among others, avoid a near-future spectrum crunch [3]. Optical Wireless Communication (OWC) is envisioned as a promising technology due to terahertz of bandwidth available in unlicensed spectrum [4] whose locally confined interference can easily be blocked by physical separators or beam adjustment, thus avoiding latency growth. Moreover, OWC technology provides a robust data transmission solution, as light is not affected by electromagnetic emissions.

Visible Light Communication (VLC) describes OWC systems in which wavelengths around 400-700 nm and Light Emitting Diodes (LEDs) used for illumination are implemented [5]. Due to the growth of high power LEDs, interest in VLC has rapidly increased to meet the sustainable and green technology paradigm, fueled by issues related to energy save and the usage of existing lighting infrastructures [6]. The advantages of this technology promote its application in areas associated with smart cities, industrial manufacturing, sub-aquatic communications, as well as in E-Health classified areas [7]–[9]. In Healhtcare environments, certain machinery can interfere with and disturb radio networks. Furthermore, RF transmission powers beyond a certain limit can amplify risks to human health [10]. In hospitals, which are sensi-

The associate editor coordinating the review of this manuscript and approving it for publication was Tianhua Xu.

tive to Electromagnetic Interference (EMI) and where high security standards are required, VLC finds a wide range of applications because it does not interfere and it is not affected by RF sources, beyond the eavesdropping prevention [10], [11]. In fact, EMI has been evaluated in a clinical laboratory by [12], who found out erroneous clinical measurements produced by such interference.

Monitoring of vital parameters such as temperature, pulse, blood pressure, respiration and electrocardiogram in IC units is extremely important for rapid and effective interventions, aimed at patients' return to baseline conditions. VLC can provide access of these parameters to doctor and/or nurse personal devices like smartphones and tablets [13]. Another important aspect is prevention and spreading of diseases, especially at this moment of worldwide situation concerning COVID-19 [14]. As most of medical equipment are connected by cables for power and network communication in a local area network (LAN), their transportation between two locations can contribute to the spread of bacteria and/or viruses. Nonetheless, research related to transmission of patients' vital signal by VLC in hospitals is relatively sparse [15], although VLC is also used as a patient-monitoring wearable device [16]. For instance, in [17] a wearable VLC device was applied on a patient-monitoring system, which used a 30 cm optical link to transmit electrocardiogram (ECG) signals from the patient in addition to On-Off-Keying (OOK) modulation. It is worth commenting that its light is perceived by human eyes, the flicker phenomenon in VLC induces physiological changes in human beings, which became one of the first effects to be studied [18]–[20]. [21]. On the other hand, the downside of some solutions using VLC is the possible interference with some medical equipment like, for instance, surgeon robots, in which infrared (IR) optical tracking systems are used [22].

OOK was used in various simulations and experimental setups to achieve a reliable and stable connection. According to the experimental work provided in [23], an uncollimated line-of-sight (LOS) link of 50 cm, with ECG data at a rate of 56 kbps, was achievable with the OOK format. In order to create a reliable ECG transmission, the authors of [24] suggested a scheme based on OOK and an 81-LED array. The authors of [25] successfully show a VLC system that transmits all vital data over a distance of 20 cm. However, the relatively short range achieved in the aforementioned works is an issue to be addressed. In [26], posturometry data was transmitted over a distance of 2 m with an OOK modulated signal at 66 Hz, whereas in [9] the authors created an OOK based prototype for patient information, resulting in an VLC LOS link over 1.3 m at a speed of 10 bps. In both cases, the low transmission rates are prohibitive in videos and/or image applications. Other modulation schemes were exploited in more complex VLC systems used to transmit ECG and ECG signals [27]–[29]. However, use of multi-parameter monitor was not considered in their works.

Manchester coding is one of the most suggested OOK line codification in low data VLC systems, as well as in Optical Camera Communication (OCC), due to reasons related to flicker, average signal intensity, among others [6]. Also due to its implementation simplicity, it is recommended in the PHY layer of such systems [35]. Therefore, it was implemented in the Ethernet 10Base-T emulation described in [30], in which commercial off-the-shelf LEDs were used in the in-line VLC system. The relatively high data rate (12.5 Mbps) was achieved in a VLC link of only 1 m. In the VLC/OCC hybrid system proposed in [31], the authors used Manchester coding in the VLC system to avoid flickering. Experimental results demonstrate the applicability of their solution in links that reach ≈6 m with relatively good performance (BER ≈ 1×10^{-3}). In [32], this line code was adopted to suppress low-frequency components of transmitted signals to alleviate bias-tee impairments. The authors demonstrate 4 Mbps indoor communication in non line-of-sight VLC links slightly farther that 1 m. The 12 kb/s OCC system evaluated in [33] also employed Manchester line code. The authors implemented an artificial neural network equalizer to increases the available bandwidth and thus enhance the data rate. Recently, the authors of [34] used a smartphone camera for indoor position with an OCC system that employed Manchester coding to guarantee an average intensity level of 50% of the maximum output power. The accuracy of their approach was confirmed in an OCC link of 2.7 m.

The feasibility of a low cost and stable Manchester-OOK based VLC system for monitoring of parameters by a multi-parametric monitor in IC units in hospitals is experimentally demonstrated here. Fig. 1 shows an illustration of the conceptual idea of implementing VLC to monitor patients in hospitals. Multi-parameter monitor data of patient located in intensive care units are transferred using illumination LEDs, and collected by smartphones of medical professionals, as well as by dongles connected to computers located in a monitoring central. Beyond the health benefits and the spectrum crunch of RF solutions, cost savings due to the employment of illumination LEDs for data communication is an important advantage of VLC in hospitals [9]. As emphasized in the on-call room depicted in Fig. 1, the application scenarios consider fixed transceivers and Line-of-Sight (LOS) links, and blockage is inconceivable in such VLC-based monitoring. Here, a setup with a prototype of a transceiver was exploited in the transmission of heart rate, oxygen saturation, pulse rate, respiration rate, temperature and non-intrusive blood pressure. The potential of the designed system was proved after a propagation in a LOS link of 15 m with an Eye Opening Penalty (EOP) of only 2.67 dB, considering an LED bias current of 400 mA and a signal frequency of 1 MHz. The performance obtained with the 1 Mbps VLC system in an indoor link of 15 m is a remarkable contribution of the present work, that demonstrates the robustness of the developed receiver prototype. Moreover, to the best of our knowledge, this is the first time that data from a multi-parameter monitor is used in VLC systems for application in hospital environments. The remainder of this paper is organized as follows. A theoretical background is presented in Section II

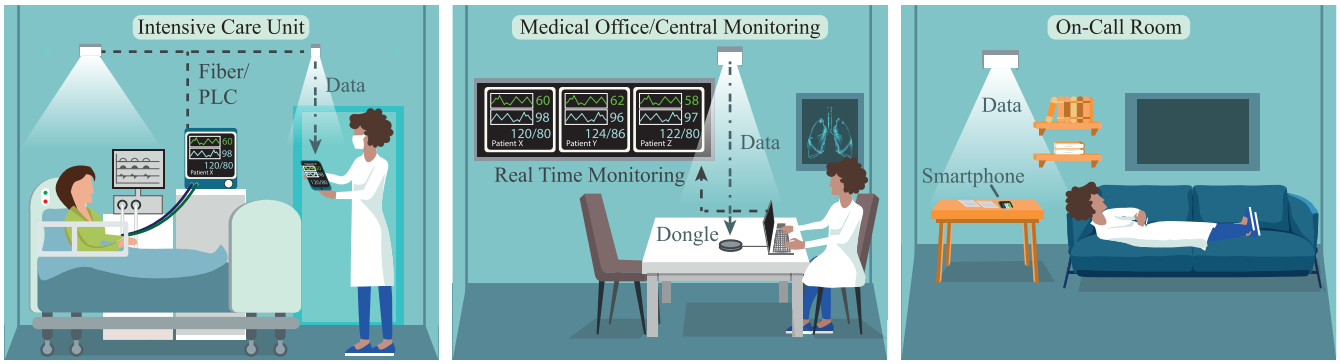

FIGURE 1. VLC-based monitoring of multi-parametric data: (i) intensive care unit; (ii) monitoring central or medical office; (iii) on-call room.

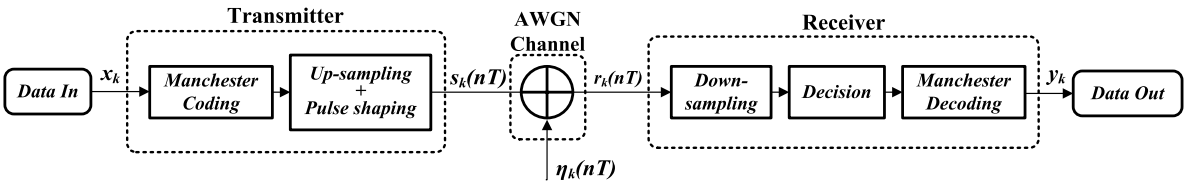

FIGURE 2. The OOK numerical model used in the signals generation and bits recovery.

and the experimental setup is described in Section III. The experimental results are discussed in Section IV, and the concluding remarks are provided in Section V.

II. THEORETICAL BACKGROUND

In this Section, we provide the basic fundamentals associated with the OOK modulation format, VLC LOS channel model and EOP metric used in the performance metrics.

A. OOK WITH MANCHESTER CODING

OOK, variable pulse-position and color-shift keying are modulation schemes recommended in the IEEE 802.15.7 standard for short-range VLC systems [19]. Implemented with specific line coding and/or scrambling methods, these schemes are able to mitigate intra-frame and inter-frame flicker [19], [35]. Also due to its simplicity and, in consequence, cost-benefit, this work focuses on the OOK format.

OOK is a type of line coding in which the generated information bits are substituted by pulses [36]. Commonly, the information bit 1 is, during the signaling interval, mapped to positive pulse, whereas the bit 0 is replaced by the absence of a pulse in an unipolar signal formulation, or by a negative pulse if bipolar signal streams are required. The simplicity of this process is requested in low cost applications, such as the one attended in the present work. Several formation laws can be used during the design of the pulses. The Manchester coding is one of the most employed due to the facilities it provides in clock recovering, while it avoids long sequences of both bits one and zero [36]. The rule that stipulates a positive pulse transition, in the middle of the duration of bit 1, and the opposite to bit 0, was adopted in this work.

Fig. 2 shows the block diagram of the numerical model used to generate and detect Manchester pulses, as well as to numerically evaluate the performance of a OOK-based VLC system through Additive White Gaussian Noise (AWGN) channels. Pseudorandom Binary Sequences (PRBS) x_k are generated for symbol mapping via Manchester codification [37]. The symbols are then up-sampled and, in sequence, pulse shaped with, for the sake of simplicity, rectangular pulses, resulting in $s_k(nT)$ modulated symbols. It is worth noting that zero mean Gaussian noise $n_k(nT)$ is added through the AWGN channel model. The received OOK signals $r_k(nT)$ are then downsampled, before a symbol recovery decision based on the average integrated signal levels. Manchester decoding can be executed by detection of one of the symbol period halves, leading to a y_k data stream.

B. THE VLC CHANNEL MODEL

Indoor VLC can be characterized as LOS and non-LOS links [38]. Nevertheless, the impairments introduced by non-LOS channels were not considered in this work, as the focus is on an LOS scenario to be deployed in the IC environments. With the available LOS, the received power can be obtained as [7]

$$P_{rLOS} = H_{LOS} \times P_t, \tag{1}$$

for P_t the average transmitted optical power and H_{LOS} the channel DC gain given by

$$H_{LOS} = \begin{cases} \dfrac{(m+1)A_r}{2\pi d^2}\cos^m(\phi)g(\psi)\cos\psi, & 0 \le \psi \le \Psi_c \\ 0, & \psi > \Psi_c \end{cases} \tag{2}$$

where m is the Lambertian emission order, A_r the photodetection area, d the transmission distance, ϕ the irradiance angle, ψ the angle of incidence, $g(\psi)$ the gain of an optical concentrator, and Ψ_c is the FOV. The Lambertian order is

associated with the LED semiangle at half-power $\Phi_{1/2}$, which is obtained as $m = \frac{\ln(2)}{\ln(\cos \Phi_{1/2})}$ [7], [38].

C. THE EOP METRIC

The Bit Error Rate (BER) evaluated by counting the difference between transmitted and received bits can become prohibitive if the communication scenario is extremely favorable. This kind of scenario belongs to the situation where the eye-diagram is well opened, demanding an estimation of the system Signal-to-Noise Ratio (SNR) through the mean and the standard deviation values of an histogram obtained from the discrete levels of eye-diagrams. However, the SNR parameter is a time-averaged indicator used most effectively when noise is the main degrading factor of a system performance. When the performance is also degraded by inter-symbol and nonlinearity distortions, the SNR estimation becomes less accurate because the popular assumption that the power density function of the received signal levels follows a Gaussian distribution is not found. In contrast, waveform distortions are taken into account by using the Eye-Opening (EO) metric, determined from the difference between the ''mark'' and ''space'' levels [39]. The eye opening penalty is the penalty of an EO, when compared to a reference EO. This reference EO is usually obtained from a back-to-back configuration, when signal waveforms are not distorted at all. In logarithmic scale, the EOP is normally given by

$$\mathrm{EOP} = 10 \times \log_{10}\left(\frac{\mathrm{EO}_{ref}}{\mathrm{EO}_{rec}}\right), \tag{3}$$

in which EO_{ref} is the eye height, i.e., the difference between the positive and negative levels of a reference signal, and EO_{rec} is the eye opening amplitude of the received signal [39]. The accuracy of the EOP calculation is assured if the detected pulses are sampled in the middle of the eye diagrams, where the EO is the widest.

III. MODEL VALIDATION THROUGH NUMERICAL SIMULATIONS

A performance evaluation in terms of BER against energy per bit to noise power spectral density ratio (E_b/N_0) was conducted in order to validate the numerical model, comparing the simulation results with values provided by a BER closed-form. Fig. 3 shows the performance comparison, considering an AWGN channel. The theoretical BER expression used in the comparison is given by

$$\mathrm{BER} = \frac{1}{2} erfc\left(\frac{E_b}{N_0}\right), \tag{4}$$

where *erfc* is the complementary error function [7]. The agreement between the simulations and the analytical results validates the numerical model.

IV. EXPERIMENTAL SETUP

Fig. 4.(a) depicts a block diagram of the experimental setup implemented to demonstrate the robustness of the VLC

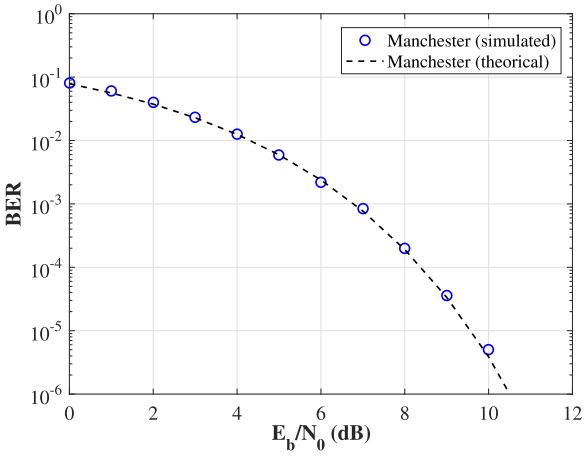

FIGURE 3. Performance comparison in terms of BER versus E_b/N_0 of the Manchester based systems in AWGN channels.

system with the frequency response shown in Fig. 5.(a). The OOK signals with Manchester codification, generated in Matlab, were loaded into a 250 MSamples/s Arbitrary Function Generator (AFG). Fig. 6 show examples of 1 MHz Manchester signals, upsampled at a rate equal to 8 samples per symbol. It can be seen in Fig. 6.(a) that long sequences of zeros and ones are prevented by the half-bit transition. Fig. 6.(b) shows slight overshoot and undershoot (ringing effect) in the signals received in the Back-To-Back (B2B) configuration. Higher frequencies encounter, as well as other effects related to impedance impairment. A signal measured after propagation in VLC system is depicted in Fig. 6.(c).

The low-pass smoothing characteristic demonstrates that the LED is one of the main system limitations in terms of bandwidth. The other main limitation is caused by the electronics coupling capacitance in an attempt to eliminate the DC component. Long sequences of ones and zeros will increase the droop phenomenon and, in worse-case, zero-out the pulse. However, in the application addressed in this work, this is not the primary concern.

The analog signals available at the AFG output were amplified to a signal amplitude of 0.3 V peak-to-peak (V_{pp}) and superimposed onto a bias current, aiming to provide non-negative waveforms. The output of the Picosecond Pulse Labs (Model 5575A, bandwidth 12 GHz, $I_{DC} \leq 500$ mA) Bias-Tee was directly supplied to the commercial LumiLED LXML-PWC2 white LED used to build the transmitter prototype shown in Fig. 4.(b). After propagation through the LOS channel, supported by bi-convex lenses, the optical signals were detected by the optical receiver prototype shown in Fig. 4.(c), before analog-to-digital conversion by a 2.5 GSamples/s Mixed Domain Oscilloscope (MDO) and offline processing of the Manchester decoding. A photo of the experimental setup is depicted in Fig. 7. The PIN used in the first stage of the photodetection is the OSRAM PIN SFH2400-Z photodiode. The second stage consists of a Transimpedance Amplifier (TIA), which employs the operational amplifier

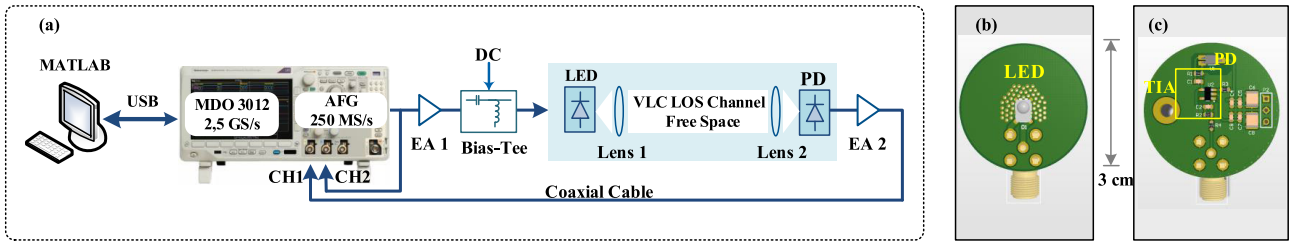

FIGURE 4. (a) Schematic view of the experimental system setup. (b) The transmitter prototype and (c) the manufactured receiver prototype.

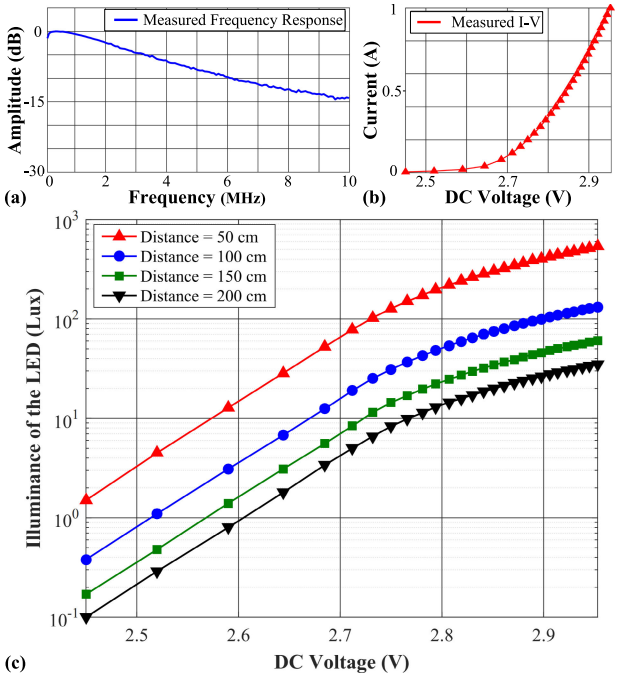

FIGURE 5. (a) Measured frequency response of the VLC system. (b) The *I-V* characteristic of the specific LED. (c) Fig. 5.(c) The *P-V* characteristic measured by a lux meter located at 50, 100, 150 e 200 cm away from the LED.

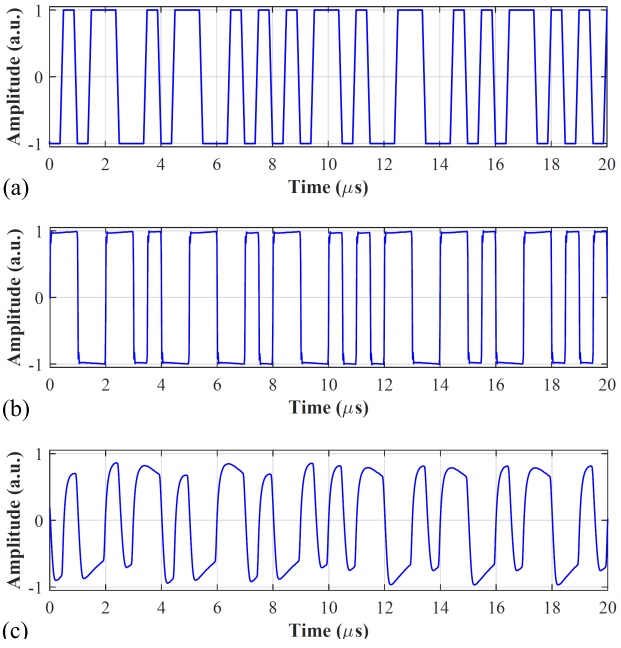

FIGURE 6. 1 MHz Manchester signals. (a) Generated using Matlab, (b) received in B2B and (c) measured after a VLC link of 1.5 m.

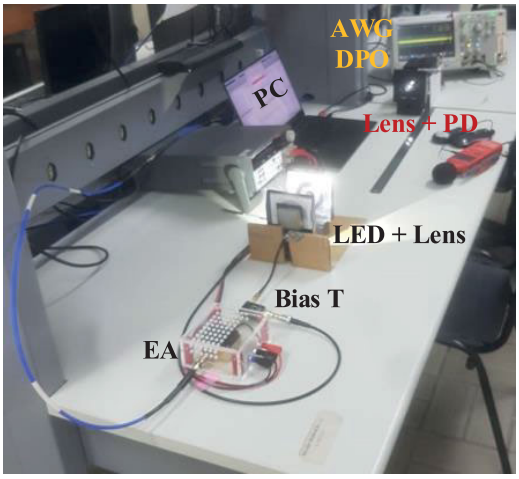

FIGURE 7. A photo of the VLC setup used in the Manchester evaluations.

LMH6629 with a bandwidth of 100 MHz and a gain of 1.8 kΩ. The third stage, composed of amplification and filtering, is desired if the amplitude of the output voltage is insufficient for a proper decodification.

Fig. 5.(b) shows the bias measured current versus the DC voltage (*I-V*) characteristics of the specific LED. Fig. 5.(c) shows *P-V* characteristic for *V* the DC or bias voltage, and *P* the illuminance obtained by a lux meter located at different distances away from the LED. Fig. 5.(c) shows that, as expected, the light intensity decreases with distance. It can also be observed from Fig. 5.(c) that with a DC voltage of $V_{bias} = 2.82$ V, the measured illuminance were 242, 59, 27.2 and 15.8 lux, at 50, 100, 150 and 200 cm, respectively.

V. EXPERIMENTAL RESULTS AND DISCUSSIONS

To resemble diverse link conditions in real IC medical environments, LOS channel lengths of 30 cm to 15 m were established and data transmission rates of 250 kbps up to 10 Mbps were covered. Furthermore, the LED drive current varied among 0-800 mA to complete a survey that displays the system optimum performance areas.

A. THE EYE-DIAGRAM USED AS REFERENCE

To establish an EOP value used as reference, a normalization process was performed by capturing the peak-to-peak amplitude in a 20 % window in the middle of the Manchester pulses. Each eye-diagram in this work consists of 9950 superimposed received symbols, divided into two symbol periods. The received signal amplitude was determined and normalized based on peak-to-peak measurement. In this work, the EOP metric is referenced on the B2B eye diagram shown in Fig. 8, which means that this eye-diagram was used as reference. It can be seen from Fig. 8 that a minor ringing effect is present, and the horizontal levels tend to rise.

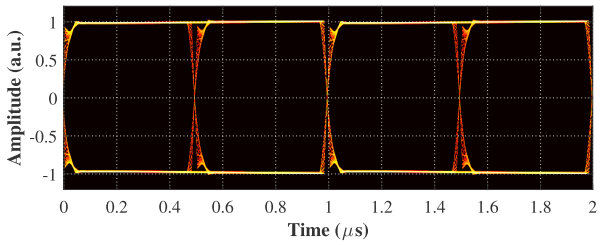

FIGURE 8. The 1 MHz Manchester eye-diagram measured in B2B.

In addition, to corroborate the adoption of the eye opening penalty as a metric in the performance evaluations, a VLC link length of 1.5 m and a signal fundamental frequency of 1 MHz were settled. Therefore, the eye diagram shown in Fig. 9.(a) can be understood as a reference eye diagram for the rest of the measurements. The two main distortions depicted in Fig. 9.(a) denote system capacitance effects, firstly exposing the LEDs' high frequency limitation on the rising and falling edges, and secondly a droop phenomenon limiting lower frequencies due to coupling capacitance. A deformation, that is caused by saturation of the receiver, elevates the eye crossing amplitude due to unbalanced positive and negative pulse duration.

To verify initial EOP results, a sample at 250 μs (the maximum EO_{ref}) and a sample at 360 μs μs (the maximum EO_{rec}) were considered. As mentioned earlier, a Gaussian distribution of the signal levels is fundamental in the implementation of the EOP metric. The histograms displayed in Fig. 9.(b1) and (b2) represent the positive and negative level distributions at the sample intervals. Although the mean of the distribution is shifted due to nonlinearities, it is possible to conclude

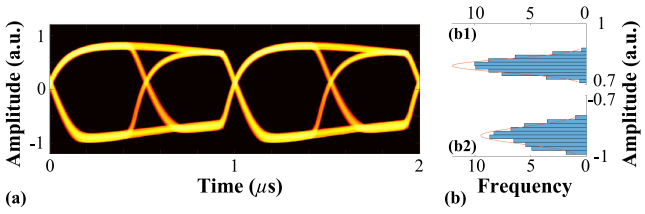

FIGURE 9. (a) The eye-diagram of the 1 MHz Manchester signals received after propagation in a VLC link of 1.5 m. (b) Distribution of the signal levels.

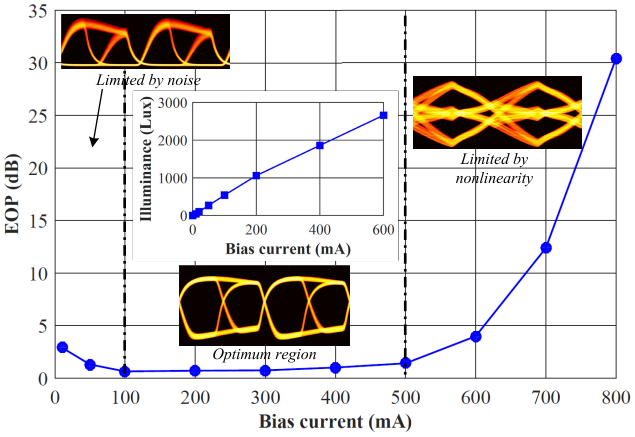

FIGURE 10. EOP as a function of the bias current I_{DC} at a distance of 1.5 m and a frequency of 1 MHz. Eye diagrams are shown as inset to emphasize the impact of signal clipping noise and LED nonlinearity.

that both levels are in conformity to the Gaussian condition. With 1.92 and 1.52 (a.u.) for EO_{ref} and EO_{rec} respectively, the obtained EOP is 1.02 dB. The error-free (absence of events with erroneous bits) eye-diagrams show that the EOP represents a good choice, in detriment of BER, to exhibit the good performance of the evaluated VLC system.

B. IMPACT OF THE LED BIAS CURRENT

It is well known that the LED bias current (I_{DC}) plays an important role in the performance of VLC systems. Performance degradation due to nonlinearities is expected when the bias current boundaries are exploited. The EOP as function of bias current, measured at 1.5 m with a frequency of 1 MHz, is shown in Fig. 10. Taking an EOP of 15 dB as a reference penalty, it is possible to verify from Fig. 10 that error-free performances are reached in the wide range of currents between 10 and ≈700 mA.

As expected, three performance regions can be established in the measured curve depicted in Fig. 10 [40]. In the first, comprising the bias currents between 0 and 100 mA, the system performance is limited by electronic and signal clipping noise [41]. In this case, the intensity of the signal is reduced, as well as the SNR, increasing thereafter the EOP. This is substantiated by the left eye diagram depicted inset Fig. 10.

An optimum performance region is verified in Fig. 10 with the currents adjusted between 100 and 500 mA. The open eye-diagram shown in the middle of 10 corroborates with this achievement. The measured illuminance versus bias current curve shown inset demonstrates the vast illuminance dynamic range (10.31 to 2260 lux), that can be explored with dimming control techniques. EOP values of 1.4 dB up to 30.39 dB, obtained at 500 and 800 mA, respectively, mark the area where the performance is affected by the LED nonlinearity [42]. The erroneous eye-diagram reproduced in the nonlinear region illustrates the impossibility of bits recovering. The bandwidth limitation of the employed LED also suggests a limit in the fundamental frequency of the Manchester pulses.

C. PERFORMANCE ANALYSIS AT DIFFERENT LINK LENGTHS

The impact of link distance in the system performance can be analyzed in Fig. 11, considering the frequencies 500 kHz, 1 MHz and 5 MHz, and the I_{DC} fixed at 400 mA. It is important to note that, in these cases, the system data rate were 500 kbps, 1 Mbps and 5 Mbps, respectively, because each information bit is represented by a rectangular pulse with amplitude equals to 1 or −1, as shown in Fig. 6.

Fig. 11 demonstrates that signals generated with the lower frequencies are less sensitive to distance, as verified by the fact that the performance results of 500 kHz and 1 MHz are nearly superimposed. The measured EOP values for 0.5 and 1 MHz were 1.03 and 0.85 dB at 50 cm, 1.08 and 0.81 dB at 5 m and 2.41 and 2.66 dB at 15 m. However, when 5 MHz is the fundamental frequency used in the Manchester signals, performance penalties around 3.14, 1.58 and 11.91 dB were registered at 0.5, 5 and 15 m, respectively, compared to the curve obtained with 1 MHz. Fig. 11 also shows outliers occurred at 1.5 m due to the photoreceiver

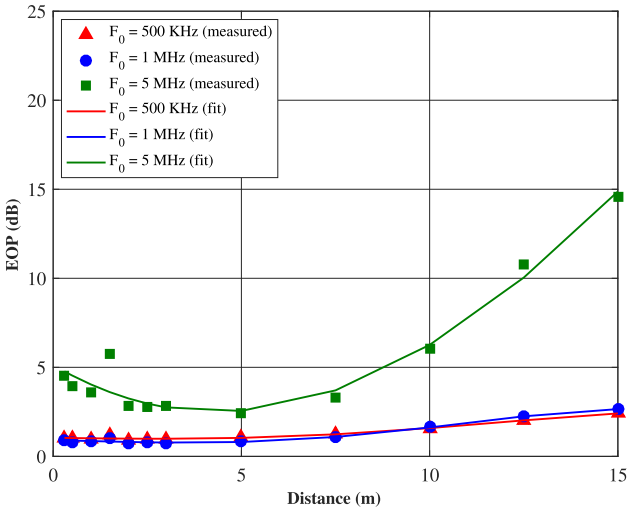

FIGURE 11. EOP as a function of the transmission distance with three different frequencies and an LED polarization current of 400 mA.

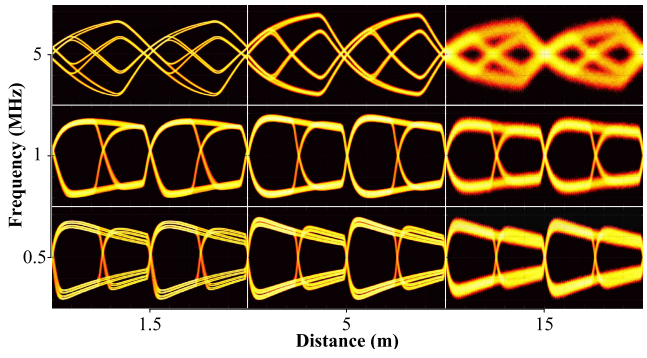

FIGURE 12. Eye diagram overview with frequency as a function of the distance, obtained at a bias current of 400 mA.

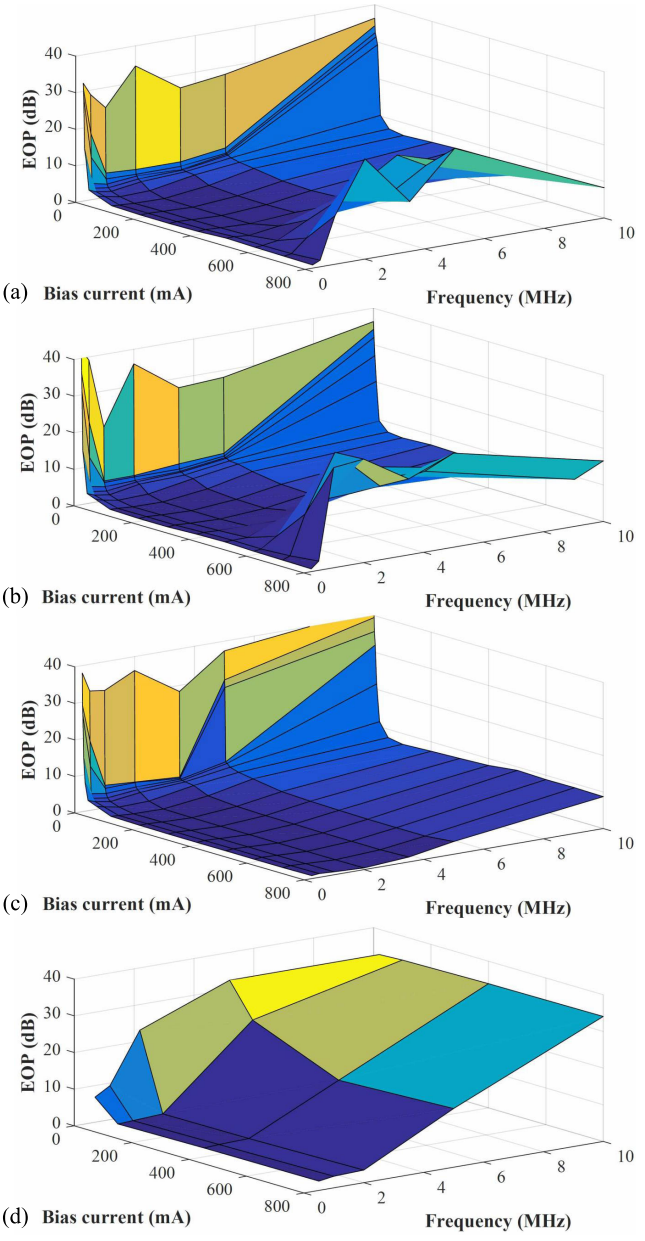

FIGURE 13. The EOP as function of both bias current and frequency. (a) At 0.5 m, (b) at 1.5 m, (c) at 3 m and (d) at 15 m.

saturation. This nonlinearity phenomenon occurs because the system was aligned at this distance. Moreover, it should be stressed that error-free measurements were achieved in almost all the results depicted in Fig. 11. The only exception occurred at 15 m, in which the measured BER was 6.62×10^{-4}. A blue-filtering normally recommended in the front of the photodetection process can be adopted to enhance this BER value [43].

An eye diagram analysis was performed to validate the signal patterns and the exploitation of the EOP metric at various link distances. An overview is shown in Fig. 12

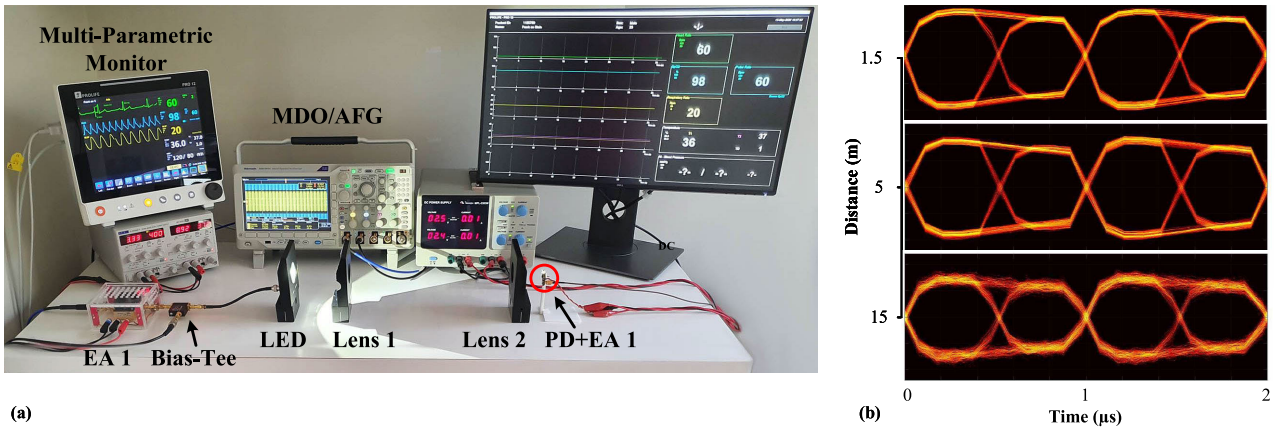

FIGURE 14. (a) A Photo of the VLC system in an E-health communication environment with a multi-parametric monitor. EA: electrical amplifier, PD: photodiode. (b) Eye-diagrams of received vital parameters at 1 MHz, 400 mA bias current and link lengths of 1.5, 5 and 15 m.

with link lengths equal to 1.5, 5 and 15 m, and frequencies of 0.5, 1 and 5 MHz. As can be seen in Fig. 12, shorter distances are impacted by nonlinearity in terms of signal level imbalance caused by the elevated light intensity and, consequently, by receiver saturation. A decrease in SNR is slightly noticeable at 5 m, unlike the significant decrease registered at 15 m, that results in the EOP of 14.57 dB shown in Fig. 11.

D. EXPLORING THE SYSTEMS OPTIMUM PERFORMANCE

Robustness is essential in a practice design of VLC system applied in IC environments in hospitals, manly due to the frequent variations in illuminance and link distance. To understand the flexibility of the design, and to actuate in the optimum operating region, a detailed survey was executed. At each distance, the EOP was measured considering various bias currents and frequencies. It should be noticed that, after the above analysis, this work focused on lower frequencies, due to the nature of the application.

It is clear from Figures 13.(a) and 13.(b) that, due to high illuminance intensity, all frequencies at distances up to 1.5 m suffer saturation distortions with currents approximately above 500 mA. However, error-free communications occurred at further distances from ≈10 up to 800 mA, with 0.5 to 3.5 MHz frequencies. As expected, the eye opening penalty increases with frequencies above 3.5 MHz and distances beyond 7.5 m. Nevertheless, a short communication link based on 10 MHz is achieved with an EOP ranging from 6.27 to 10.69 dB, for VLC link lengths between 0.3 and 5 m.

Typical VLC channels in hospitals can be established directed downwards from the ceiling and in some cases directed from walls, which leads to distances between 1 and 3 m. Nevertheless, the results presented in Fig. 13.(c) and Fig. 13.(d) prove that the VLC system evaluated here can also be applied in relatively long range environments, with a dimming range around 10 up to 700 mA, and at a cost of signal frequency reduction.

E. EXPERIMENTAL RESULTS WITH THE MULTI-PARAMETER MONITOR

Finally, the developed prototype was examined in the health-care setup depicted in Fig. 14.(a). Accordingly, a multi-parameter PRO12 monitor was used to resemble an E-health communication environment. This monitor captures vital parameters, such as heart rate, oxygen saturation, pulse rate, respiration rate, temperature and non-intrusive blood pressure, and utilizes the HL7 protocol for data communication [44]. Since the HL7 protocol is limited, the transmitted data was used for trend analysis with a central monitoring system applied in hospitals. The data acquisition was executed every second over a LAN connection and sent to a local HL7 server, and then prepared for VLC transmission through the evaluated setup.

It is worth noting that the setup depicted in Fig. 14.(a) is based on the diagram of Fig. 4, with a multi-parametric meter. In the data reception, a simple form of checksum is executed on the data, which contains information related to heart rate and respiration rate based on a ECG-measurement. Likewise, an oxygen saturation (SPO_2), a pulse rate based on SPO_2 and a temperature measurement belong to the 1 Hz data string. The non-invasive blood pressure measurement is sent separately, after the execution of the other measurement.

It is also important to notice that, despite its absence in Fig. 14.(a), the information captured in Matlab was used to generate the OOK signals based on Manchester coding, which served as electrical modulating signals in the optical modulation process. This means that the codified pulses were offline generated using a fundamental frequency of 1 MHz, and the analog signals provided at the output of the AFG modulated the LED. Due to the provision of 420 symbols up-sampled at 8 to 3360 samples in total, the oscilloscopes parameters and settings with a resolution of 10 samples per symbol were achieved and shown in Fig. 14.(b).

The captured vital parameters were sent considering an LED polarization current of 400 mA, at VLC distances of 1.5, 5 and 15 m. Fig. 14.(b) shows eye diagrams of the received

signals with all evaluated distances. As can be observed in Fig. 14.(b), the already down-sampled signals at the data reception present a slight deviation in the final eye opening penalty. However, the obtained results follow the line of the earlier experimental results of Fig. 11, where 1.02, 0.83 and 2.66 dB were achieved at 1.5, 5 and 15 m, respectively. Results with the multi-parameter monitor provide EOP values equal to 0.89, 0.96 and 2.67 dB at the equivalent distances.

VI. CONCLUSION

The feasibility of a low cost and stable Manchester-OOK based visible light communication (VLC) system for application in intensive care medical environments was experimentally demonstrated in this work. The transmitter and the receiver parts of a VLC transceiver were designed, manufactured and properly characterized before performance evaluations with measurements of the eye opening penalty metric. The impact of the LED bias current, as well as the modulation frequency and line-of-sight link distance was extensively analyzed. The experimental results show an outstanding behavior considering an LED bias current of 400 mA, a signal frequency of 1 MHz, and a VLC transmission link of 2.5 m.

A proof-of-concept based on an experimental apparatus was prepared for parameter monitoring using a multi-parameter monitor with the following signals: heart rate, oxygen saturation, pulse rate, respiration rate, temperature and non-intrusive blood pressure. Considering an LED polarization current of 400 mA, EOP values of 0.89, 0.96 dB were measured at VLC links of 1.5, 5 m respectively. We can conclude, based on the eye opening penalty of only 2.67 dB achieved in the VLC link of 15 m, that the VLC system evaluated here presents itself as a potential technology for application in classified areas like intensive care medical units in hospitals.

REFERENCES

[1] J. Navarro-Ortiz, P. Romero-Diaz, S. Sendra, P. Ameigeiras, J. J. Ramos-Munoz, and J. M. Lopez-Soler, "A survey on 5G usage scenarios and traffic models," *IEEE Commun. Surveys Tuts.*, vol. 22, no. 2, pp. 905–929, 2nd Quart., 2020.

[2] H. Viswanathan and P. E. Mogensen, "Communications in the 6G era," *IEEE Access*, vol. 8, pp. 57063–57074, 2020.

[3] S. Baig, H. M. Asif, T. Umer, S. Mumtaz, M. Shafiq, and J. Choi, "High data rate discrete wavelet transform-based PLC-VLC design for 5G communication systems," *IEEE Access*, vol. 6, pp. 52490–52499, 2018.

[4] M. Z. Chowdhury, M. K. Hasan, M. Shahjalal, M. T. Hossan, and Y. M. Jang, "Optical wireless hybrid networks: Trends, opportunities, challenges, and research directions," *IEEE Commun. Surveys Tuts.*, vol. 22, no. 2, pp. 930–966, 2nd Quart., 2020.

[5] H. Haas, L. Yin, Y. Wang, and C. Chen, "What is LiFi?" *J. Lightw. Technol.*, vol. 34, no. 6, pp. 1533–1544, Mar. 15, 2016.

[6] S. Arnon, *Visible Light Communication*. Cambridge, U.K.: Cambridge Univ. Press, 2015.

[7] Z. Ghassemlooy, L. N. Alves, S. Zvanovec, and M.-A. Khalighi, *Visible Ligh Communications: Theory and Applications*. Boca Raton, FL, USA: CRC Press, 2017.

[8] P. W. Berenguer, D. Schulz, J. Hilt, P. Hellwig, G. Kleinpeter, J. K. Fischer, and V. Jungnickel, "Optical wireless MIMO experiments in an industrial environment," *IEEE J. Sel. Areas Commun.*, vol. 36, no. 1, pp. 185–193, Jan. 2018.

[9] W. A. Cahyadi, T.-I. Jeong, Y.-H. Kim, Y.-H. Chung, and T. Adiono, "Patient monitoring using visible light uplink data transmission," in *Proc. Int. Symp. Intell. Signal Process. Commun. Syst. (ISPACS)*, Nov. 2015, pp. 431–434.

[10] L. U. Khan, "Visible light communication: Applications, architecture, standardization and research challenges," *Digit. Commun. Netw.*, vol. 3, no. 2, pp. 78–88, May 2016.

[11] V. P. Rachim, Y. Jiang, H.-S. Lee, and W.-Y. Chung, "Demonstration of long-distance hazard-free wearable eeg monitoring system using mobile phone visible light communication," *Opt. Exp.*, vol. 25, no. 2, pp. 713–719, 2017.

[12] N. D. Badizadegan, S. Greenberg, H. Lawrence, and K. Badizadegan, "Radiofrequency interference in the clinical laboratory: Case report and review of the literature," *Amer. J. Clin. Pathol.*, vol. 151, no. 5, pp. 522–528, 2019.

[13] V. P. Rachim, J. An, P. N. Quan, and W.-Y. Chung, "A novel smartphone camera-LED communication for clinical signal transmission in mHealth-rehabilitation system," in *Proc. 39th Annu. Int. Conf. IEEE Eng. Med. Biol. Soc. (EMBC)*, Jul. 2017, pp. 3437–3440.

[14] M. A. Rahman, M. S. Hossain, N. A. Alrajeh, and N. Guizani, "B5G and explainable deep learning assisted healthcare vertical at the edge: COVID-I9 perspective," *IEEE Netw.*, vol. 34, no. 4, pp. 98–105, Jul. 2020.

[15] J. An and W. Chung, "Wavelength-division multiplexing optical transmission for EMI-free indoor fine particulate matter monitoring," *IEEE Access*, vol. 6, pp. 74885–74894, 2018.

[16] T. Adiono, R. F. Armansyah, S. S. Nolika, F. D. Ikram, R. V. W. Putra, and A. H. Salman, "Visible light communication system for wearable patient monitoring device," in *Proc. IEEE Region Conf. (TENCON)*, Nov. 2016, pp. 1969–1972.

[17] M. Mayuri, B. Vijayalakshmi, and K. Sindhubala, "Biomedical data transmission using visible light communication," *Int. J. Appl. Eng. Res.*, vol. 10, no. 20, pp. 1–5, 2015.

[18] S. Rajagopal, R. Roberts, and S.-K. Lim, "IEEE 802.15.7 visible light communication: Modulation schemes and dimming support," *IEEE Commun. Mag.*, vol. 50, no. 3, pp. 72–82, Mar. 2012.

[19] *IEEE Standard for Local and Metropolitan Area Networks—Part 15.7: Short-Range Wireless Optical Communication Using Visible Light* Standard 802.15.7-2018, 2011.

[20] C. E. Mejia, C. N. Georghiades, M. M. Abdallah, and Y. H. Al-Badarneh, "Code design for flicker mitigation in visible light communications using finite state machines," *IEEE Trans. Commun.*, vol. 65, no. 5, pp. 2091–2100, May 2017.

[21] S. S. Torkestani, S. Sahuguede, A. Julien-Vergonjanne, and J. P. Cances, "Indoor optical wireless system dedicated to healthcare application in a hospital," *IET Commun.*, vol. 6, no. 5, pp. 541–547, Mar. 2012.

[22] S. M. Mana, P. Hellwig, J. Hilt, K. L. Bober, V. J. Hirmanova, P. Chvojka, R. Janca, and S. Zvanovec, "LiFi experiments in a hospital," in *Proc. Opt. Fiber Commun. Conf. (OFC)*, Mar. 2020, pp. 1–3.

[23] Y.-K. Cheong, X.-W. Ng, and W.-Y. Chung, "Hazardless biomedical sensing data transmission using VLC," *IEEE Sensors J.*, vol. 13, no. 9, pp. 3347–3348, Sep. 2013.

[24] D. R. Dhatchayeny, A. Sewaiwar, S. V. Tiwari, and Y. H. Chung, "Experimental biomedical EEG signal transmission using VLC," *IEEE Sensors J.*, vol. 15, no. 10, pp. 5386–5387, Oct. 2015.

[25] C. U. Kumari and S. Dhanalakshmi, *All Optical Health Monitoring System: An Experimental Study on Visible Light Communication in Biomedical Signal Transmission*. Singapore: Springer, 2018, pp. 361–370.

[26] Y. F. Luckyarno, P. Cherntanomwong, and R. Wijaya, "Posturometry data transmission using visible light communication," in *Proc. 13th Int. Conf. Electr. Eng./Electron., Comput., Telecommun. Inf. Technol. (ECTI-CON)*, Jun. 2016, pp. 1–4.

[27] C. Huang and X. Zhang, "Impact and feasibility of darklight LED on indoor visible light positioning system," in *Proc. IEEE 17th Int. Conf. Ubiquitous Wireless Broadband (ICUWB)*, Sep. 2017, pp. 1–5.

[28] D. Ilakkiaselvan, K. Naveen, M. Veerasekar, and S. Ponnaiah, "Real time biomedical signal transmission using visible light communication," *Int. Res. J. Latest Trends Eng. Technol.*, vol. 3, no. 1, pp. 1–8, 2016.

[29] W. Ding, F. Yang, H. Yang, J. Wang, X. Wang, X. Zhang, and J. Song, "A hybrid power line and visible light communication system for indoor hospital applications," *Comput. Ind.*, vol. 68, pp. 170–178, Apr. 2015.

[30] A. Sturniolo, G. Cossu, A. Messa, and E. Ciaramella, "Ethernet over commercial lighting by a visible light communication," in *Proc. Global LIFI Congr.*, Feb. 2018, pp. 1–4.

[31] D. T. Nguyen, S. Park, Y. Chae, and Y. Park, "VLC/OCC hybrid optical wireless systems for versatile indoor applications," *IEEE Access*, vol. 7, pp. 22371–22376, 2019.
[32] Y. Zhu, C. Gong, J. Luo, Z. Xu, and W. Xu, "SVM-assisted realization and demonstration of indoor 4 Mb/s non-line-of-sight visible light communication with second-order reflection," *IEEE Photon. J.*, vol. 11, no. 5, pp. 1–17, Oct. 2019.
[33] O. I. Younus, N. Bani Hassan, Z. Ghassemlooy, P. A. Haigh, S. Zvanovec, L. N. Alves, and H. Le Minh, "Data rate enhancement in optical camera communications using an artificial neural network equaliser," *IEEE Access*, vol. 8, pp. 42656–42665, 2020.
[34] M. Rego and P. Fonseca, "OCC based indoor positioning system using a smartphone camera," in *Proc. IEEE Int. Conf. Auto. Robot Syst. Competitions (ICARSC)*, Apr. 2021, pp. 31–36.
[35] Z. Wang, Q. Wang, Z. Xu, and W. Huang, *Visible Light Communications: Modulation and Signal Processing*. Hoboken, NJ, USA: Wiley, 2017.
[36] J. Proakis and M. Salehi, *Digital Communications*, vol. 4. New York, NY, USA: McGraw-Hill, 2001.
[37] *IEEE Standard for Ethernet*, Standard 802.3-2018 (Revision of IEEE Std 802.3-2015), 2018, pp. 1–5600.
[38] J. M. Kahn and J. R. Barry, "Wireless infrared communications," *Proc. IEEE*, vol. 85, no. 2, pp. 265–298, Feb. 1997.
[39] L. Binh, *Optical Fiber Communication Systems With MATLAB and Simulink Models in*. Boca Raton, FL, USA: CRC Press, 2014.
[40] R. B. Nunes, H. R. de O. Rocha, M. E. V. Segatto, and J. A. L. Silva, "Experimental validation of a constant-envelope OFDM system for optical direct-detection," *Opt. Fiber Technol.*, vol. 20, no. 3, pp. 303–307, 2014.
[41] K. M. vd Zwaag, J. L. C. Neves, H. R. O. Rocha, M. E. V. Segatto, and J. A. L. Silva, "Adaptation to the LEDs flicker requirement in visible light communication systems through CE-OFDM signals," *Opt. Commun.*, vol. 441, pp. 14–20, Jun. 2019.
[42] K. vd Zwaag, J. Neves, H. Rocha, M. Segatto, and J. Silva, "Increasing VLC nonlinearity tolerance by CE-OFDM," in *Proc. Latin Amer. Opt. Photon. Conf.*, Nov. 2018, Paper W3D-3.
[43] M. Khadr, A. A. El Aziz, H. Fayed, and M. Aly, "Bandwidth and BER improvement employing a pre-equalization circuit with white LED arrays in a MISO VLC system," *Appl. Sci.*, vol. 9, no. 5, p. 986, Mar. 2019.
[44] H. International. (2020). *Health Level 7 Standard*. Accessed: Apr. 8, 2020. [Online]. Available: https://www.hl7.org/index.cfm

KLAAS MINNE VAN DER ZWAAG received the M.S. degree in electrical engineering from the Federal University of Espírito Santo (UFES), Vitória, Brazil. His research interests include modulation formats, VLC, and the IoT.

MARIANNE PONTARA MARINHO is currently pursuing the bachelor's degree in electrical engineering with the Federal University of Espírito Santo (UFES), Vitória, Brazil. Her research interests include modulation formats and VLC systems.

WESLEY DA SILVA COSTA is currently pursuing the D.S. degree in electrical engineering with the Federal University of Espírito Santo (UFES), Vitória, Brazil. His research interest includes advanced modulation formats in VLC systems.

FRANCISCO DE ASSIS SOUZA DOS SANTOS received the M.S. and Ph.D. degrees in electrical engineering from the Federal University of Santa Catarina, Brazil. He joined the Department of Computing and Electronic, Federal University of Espírito Santo (UFES), Vitória, Brazil.

TEODIANO FREIRE BASTOS-FILHO received the B.S. degree in electrical engineering from the Federal University of Espírito Santo (UFES), Vitória, Brazil, and the Ph.D. degree in physical sciences from the Universidad Complutense de Madrid. He is currently a Full Professor at UFES.

HELDER R. O. ROCHA received the B.S. degree in electrical engineering and the M.S. and D.S. degrees in computing science from the Federal University of Fluminense, Brazil. He joined the Department of Electrical Engineering, Federal University of Espírito Santo (UFES), Vitória, Brazil. His research interest includes system optimization.

MARCELO E. V. SEGATTO received the B.S. degree in electrical engineering from the Federal University of Espírito Santo (UFES), Vitória, Brazil, the M.Sc. degree in telecommunications from the Universidade Estadual de Campinas, Brazil, and the Ph.D. degree from the Imperial College of London. He joined the Department of Electrical Engineering, UFES. His main research interests include fiber-optic communication systems, sensors, and networks.

JAIR A. L. SILVA (Member, IEEE) received the B.S., M.S., and Ph.D. degrees in electrical engineering from the Federal University of Espírito Santo (UFES), Vitória, Brazil. He joined the Department of Electrical Engineering, UFES. His research interests include 5G, the IoT, optical fiber communication, and advanced modulation formats.